Proceedings of the Canadian Society for Mechanical Engineering International Congress 2022
CSME Congress 2022
June 5-8, 2022, Edmonton, AB, Canada

Optimizing Print Parameters for Maximizing Tensile Strength of Additively Manufactured Polymers Through Evolutionary Algorithms

N. Nguyen, B. Sanderson, S. Molazadeh, A. Hosseini*, H.A. Kishawy, S. Rahnamayan
Faculty of Engineering and Applied Science, Ontario Tech University, Oshawa, Canada
*sayyedali.hosseini@ontariotechu.ca

***Abstract*—**Additive Manufacturing (AM) has been adopted worldwide for rapid prototyping and small-scale production of complex parts. Despite its widespread adoption, much is still unknown about AM. Many researchers have devoted significant e fforts t o studying the importance of AM characteristics such as build time, dimensional accuracy, surface quality, and mechanical behavior in relation to the printing parameters used to create them. Several research have indicated the impacts of printing parameters on the performance of fused filament fabrication (FFF); however, developing a generic model to optimize FFF printing parameters received little attention. This study presents the utilization of genetic programming along with a genetic algorithm to search for the best set of printing parameters that maximizes the tensile strength of PLA samples. The search variables are raster angle, extrusion width, and extrusion temperature. From the test results, genetic programming using Eureqa is conducted to obtain a surrogate model that predicts tensile strength from print parameters. Finally, a genetic algorithm is used to obtain the set of printing parameters that maximizes tensile strength of the test specimen. The proposed model showed a good agreement with experimental data.

***Keywords*—3D printing, additive manufacturing, fused filament fabrication, genetic algorithm, genetic programming, tensile strength.**

I. Introduction

Additive manufacturing (AM) is a manufacturing technology that allows a component to be generated from a 3D model with minimal post-processing. Consequently, AM allows designers to create unique or sophisticated models in a single step without the constraints of traditional production, such waste management, difficulty generating complex geometries, or the need for specialized equipment [1]. Since the late 1980s, AM has advanced in technology and has become widely adopted in the last ten years. While AM applications will continue to expand, its benefits have already had a significant impact on five industries: aerospace, consumer goods, energy, healthcare, and transportation [2]. AM sees most of its use in short-run part production and rapid prototyping. AM processes include directed energy deposition, material extrusion, material jetting, powder bed fusion, etc. Polymers, ceramics, and metals are the predominant materials that are used in AM processes [3].

Optimization methods can help researchers generate models to overcome the design and process flaws in AM and link the AM process parameters to material and structural properties. Topology optimization and process variable optimization are widely used to design the optimal part geometry, support structure, and process parameters [4]. Different optimization techniques such as Analysis of variance (ANOVA), Genetic algorithm (GA), Particle swarm optimization (PSO), Taguchi, and hybrid methods have been introduced to propose the optimal printing parameters [5].

The tensile strength of an FFF printed part is the most explored and analyzed attribute. Prior research has shown that build orientation and raster angle are the most influential process parameters regarding the tensile strength of FFF produced parts.

This paper begins with a background of AM and an introduction of the current state of the art in using optimization techniques with AM technologies. In addition, genetic algorithm (GA) and genetic programming (GP) process are explained. Section III explains the proposed optimization scheme for optimizing print parameters. Section IV explains the experimentation required for this optimization. Finally, section V reports the results of the experiments and optimization.

II. Background

A. Additive Manufacturing

Fused filament fabrication (FFF) is a solid-extrusion based 3D printing process that was invented by Stratasys in early 1992 was initially used to make prototypes. The layers are created by extruding a thermoplastic (ABS, PLA, etc.) through a heated nozzle to print one cross-section of an item, and then repeating the process as layers to complete the part. The anisotropic mechanical properties of FFF printed parts have attracted much interest in recent years. The impact of FFF build variables on stiffness, strength, and fracture performance has been investigated. ASTM D638 test techniques for tensile performance of plastics are used for most of the fundamental tensile testing, which studies the influence of process variables on tensile strength. The influences of raster orientation, air gap, extrusion width, colour, and print temperature on the tensile and compressive strengths of directionally manufactured specimens were investigated by Ahn and colleagues [6]. Riddick et al. [7] used tensile testing to assess the mechanical properties of the FFF process parameters like build direction and raster orientation. Huang and Singamneni [8] utilized the tensile test as the experimental setup to study the impact of raster angle on modulus and strength in FFF components.

Many researchers have developed different approaches to optimize the mechanical properties of FFF parts and process parameters. Ulu, et al. [9] proposed the surrogate-based optimization approach to improve structural performance by evaluating mechanical property sensitivities and optimizing build orientation. They used tensile testing as the experimental setup for obtaining the mechanical and material properties. Torres et al. [10] have developed a method for optimizing FFF mechanical properties based on experimental sensitivity to build parameters such as layer thickness, density, extrusion temperature, speed, infill direction, and component orientation. Wang et al. [11] used a genetic algorithm to obtain the optimum printing direction. Nguyen et al. [12] investigated the optimal set of FFF process parameters by using NSGA-II algorithm.

B. Genetic Algorithm

First developed by John Holland in 1975 [13], GA is a category of evolutionary algorithms used to find optimal solutions to problems by mimicking the natural selection process. GA involves manipulating a population of "chromosomes," whereby each chromosome encodes the variable values of the problem to be solved. Chromosomes that return better results in an optimization problem will have a higher chance of crossover to create offspring and pass on their desirable characteristics to the next generations. This process happens over many generations until an acceptable optimization result is found.

1) Chromosome Encoding: Chromosomes are discrete binary strings that contain only 0s and 1s. Encoding allows the chromosomes to represent values within any specified range. A string of 0s means that the variable is at the minimum value, while a string of 1s means the variable is at the maximum value.

2) Objective Function and Fitness Evaluation: The objective is to find a combination of print parameters to maximize the tensile strength. Raster angle, extrusion width, extrusion temperature, and ultimate strength are α, w, T, and σ_{UTS}, respectively. The objective function is in the form of (1).

$$f(a, w, T) = max\left\{\sigma_{UTS}\right\} \tag{1}$$

Fitness evaluation determines the probability of choosing a chromosome as one of the crossover parents. A higher objective function value will lead to higher selection probability for crossover. Parents were selected based on their fitness scores using roulette wheel selection. There are various methods of assigning a selection probability from evaluation scores, such as proportionate reproduction [14], ranking selection [15], tournament selection [16], or Genitor selection [17]. This paper utilized a simple linear selection probability increase based on ranking. The population size is 100; thus, the selection probability starts at zero for the worst individual, then increases linearly by 0.0202% as individual ranking increases, up to 2% for the best individual.

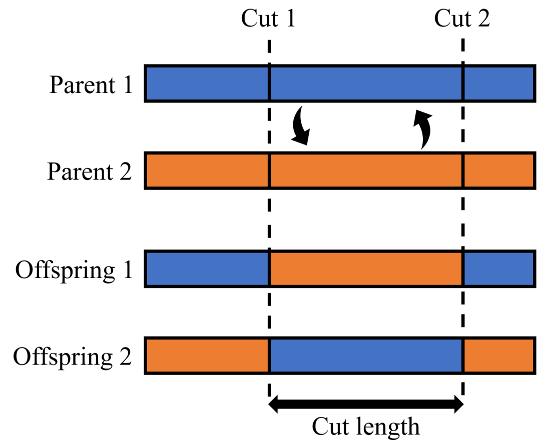

Figure 1. Illustration of two-point crossover.

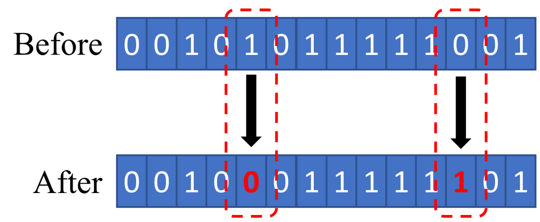

Figure 2. Mutation operation.

3) Biological Operators: Crossover is a process that involves two or more chromosomes. These chosen chromosomes are called parents. Offspring are created by recombining the binary strings of the parents randomly.

In this paper, a two-point crossover is utilized. Two cut locations are chosen at random. The binary segment between the cut points is swapped between the parents, and the resulting new chromosomes are offspring, as shown in Fig. 1. In addition, to reduce the likelihood that the crossover operation creates clones of the parents, the distance between the two cut locations (cut length) is set to a minimum of 5 bits. Random cloning happens when the swapping segment are identical, which is more likely to happen if the cut length is small.

After crossover, the mutation procedure is performed. The cloned elites are likewise subjected to the mutation procedure. Mutation occurs when the binary bits of the chromosomes are flipped.

C. Genetic Programming

GP was invented and patented by Koza in 1990 [18] as an extension of GA. It was developed to solve problems beyond optimizing values, where fundamental system modelling is required. GP shares many similarities with GA; they are both population-based evolutionary algorithms, with selection, crossover, and mutation operations. The primary difference between GP and GA is the structure of the individual. Each

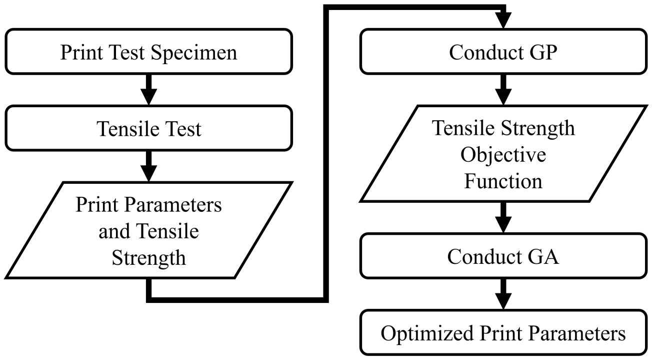

Figure 3. Optimization procedure flowchart.

individual for GP is a computer program or an equation, while each individual in GA is a binary string or a vector of values. In addition, the chromosome size of GP changes over time as equation complexity increases; meanwhile, the chromosome size for GA stays constant.

III. Proposed Scheme

The proposed procedure in this paper involves the utilization of both GA and GP to obtain the best 3D printing parameters, as shown in Fig. 3.

GA is a population-based algorithm; thus, printing test specimens for each individual in GA would be prohibitively expensive. 3D printing and tensile test simulations are also very computationally expensive. GP is used to create a surrogate model that can effectively predict tensile strength from 3D printing parameters. GP surrogate model is obtained by printing 27 tensile tests, where each test specimen is printed using a unique combination of printing parameters. The printing parameter combinations and the resulting tensile strengths from tensile tests form the database for GP to search for the optimization function. Finally, GA is used to obtain the optimized printing parameters according to the surrogate model.

All evolutionary algorithm (EA), which includes GA and GP, follows a closed-loop until either a satisfactory result has been reached or a limited number of generations has been reached.

A. Genetic Programming Implementation

Implementing GP is done using Eureqa [19]. The GP search building blocks and trigonometric functions to regulate the raster angle parameter enables the most basic mathematical operations. In addition, exponential, natural logarithm, and power are included, at lower complexity, as shown in Table I. The stop criteria for the GP is a R2 goodness of fit of 0.95.

$$R^2 = 1 - \frac{SS_{residual}}{SS_{total}} \tag{2}$$

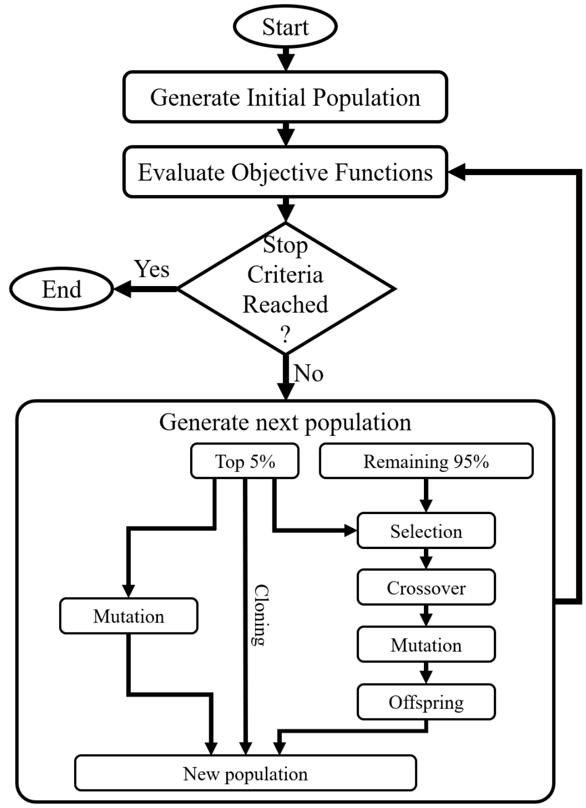

Figure 4. GA evolutionary algorithm flowchart.

TABLE I
GP formula building blocks using Eureqa

Building-blocks	Complexity	Building-blocks	Complexity
Constants	1	Sine	3
Input variable	1	Cosine	3
Addition	1	Exponential	4
Subtraction	1	Natural logarithm	4
Multiplication	1	Power	5
Division	1		

B. Genetic Algorithm Application

GA implementation is done using MATLAB. GA starts with a uniform, randomly generated population of 100 individuals. This population size is maintained through all generations. For each generation, each individual's fitness is evaluated by calculating the predicted tensile strength from printing parameters according to the GP surrogate model. Then the individuals are ranked from highest tensile strength to lowest. Their probability of being chosen as one of the parents for crossover is calculated based on their ranking in the population. Elitism ensures that the best genes are not lost, where five best performing individuals are allowed to propagate directly to the next generation. In addition, these five elites are also cloned and mutated before going to the next generation. Both the cloned elites and the offspring from crossover experience a mutation rate of 5%. Finally, all individuals in the new

TABLE II
GA CONTROL PARAMERS

Parameters	Value
Population size	100
Elitism rate	5%
Crossover rate	90%
Mutation rate	5%
Maximum number of generations	100
Chromosome total binary bits length	60
Binary bits length for each variable	20
Stop criteria	100 iterations

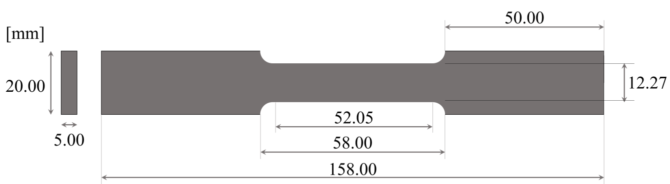

Figure 5. Tensile specimen dimensions.

population are evaluated, and a new iteration starts. GA parameters are encapsulated in Table II. At the end of a GA search, optimized printing parameters are obtained.

IV. Experiment Design and Tests

A. Material and Specimen

Polylactic acid (PLA) was selected as the material studied in this paper. The samples were created from white 1.75 mm PLA manufactured by 3D Printing Canada. The specimens were fabricated on a Voxelab Aquila FFF 3D printer. The open-source software Ultimaker Cura was used to slice the tensile 3D model, control the printing process parameters, and generate the G-Code for use in the printer. The tensile specimens were prepared in the conventional "dog bone" style, and the dimensions are shown in Fig. 5. The specimens were printed solid with no cavities or infill to reduce extraneous factors.

B. Process Parameters

Three variables were selected for analysis, with three variations each for 27 combinations. Each specimen has two walls surrounding the perimeter to aid printing. The walls are only changed between trials by extrusion width. The specimens consist of 50 layers, with a layer height of 0.1 mm. All parameters aside from the three search variables remained constant between samples.

TABLE III
PRINTING PARAMETER BOX-CONSTRAINTS.

Variable	Min	Max
Raster Angle	0°	90°
Extrusion Width	0.4 mm	0.6 mm
Extrusion Temperature	200°C	220°C

TABLE IV
TENSILE TEST RESULTS

Test No.	Raster Angle (degrees)	Ex. Width (mm)	Ex. Temp. (°C)	UTS (MPa)
1	0	0.4	200	28.883
2	0	0.5	200	9.6389
3	0	0.6	200	13.244
4	45	0.4	200	34.475
5	45	0.5	200	39.417
6	45	0.6	200	28.242
7	90	0.4	200	49.052
8	90	0.5	200	54.16
9	90	0.6	200	53.494
10	0	0.4	210	25.546
11	0	0.5	210	31.956
12	0	0.6	210	12.705
13	45	0.4	210	36.638
14	45	0.5	210	25.175
15	45	0.6	210	26.357
16	90	0.4	210	54.773
17	90	0.5	210	53.588
18	90	0.6	210	53.897
19	0	0.4	220	31.127
20	0	0.5	220	20.982
21	0	0.6	220	26.535
22	45	0.4	220	45.367
23	45	0.5	220	36.211
24	45	0.6	220	41.475
25	90	0.4	220	50.277
26	90	0.5	220	51.848
27	**90**	**0.6**	**220**	**57.161**

C. Testing Procedure

Once the specimens were fabricated, their tensile performance was evaluated in a LS100Plus 100 kN Universal Materials Testing Machine. The specimens were secured in the jaws and pulled at 40 mm/min, stopping at fracture. The ultimate tensile strength (UTS) was calculated using force at fracture and cross-sectional area.

V. Results and Discussion

A. Testing Results

Table IV list all tensile tests and their varying strengths. The average UTS was 36.75 MPa, with a maximum of 57.16 MPa and a minimum of 9.64 MPa. The specimen printed at 220°C with a 90-degree infill direction and 0.6 mm extrusion width achieved the highest UTS. The sample with the minimum UTS has a temperature, extrusion width, and raster angle of 200°C, 0.5 mm, and 0 degrees, respectively. Process variables have a considerable impact on sample strength.

B. Parameter Correlation

Fig. 6a, Fig. 6b, and Fig. 6b show the effects of raster angle, extrusion width, and extrusion temperature, respectively. Raster angle has the strongest correlation with increasing strength, demonstrated by the upwards trend. Extrusion width has a negligible effect on the strength directly, but consistency appears to decrease as the extrusion width increases, as shown by the tight grouping at 0.4 mm and the spread at 0.6 mm. Extrusion temperature shows a slight increase in strength

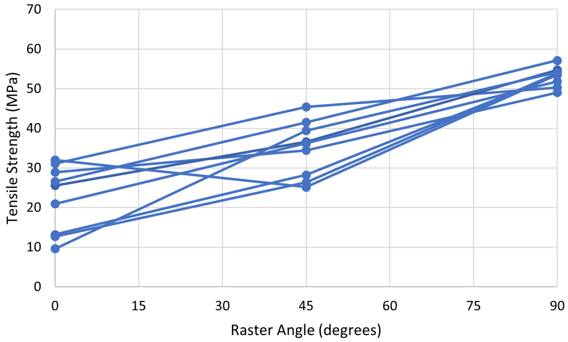

(a) Tensile strength versus raster angle

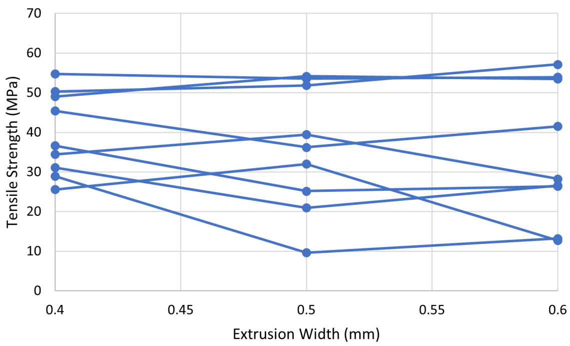

(b) Tensile strength versus extrusion width

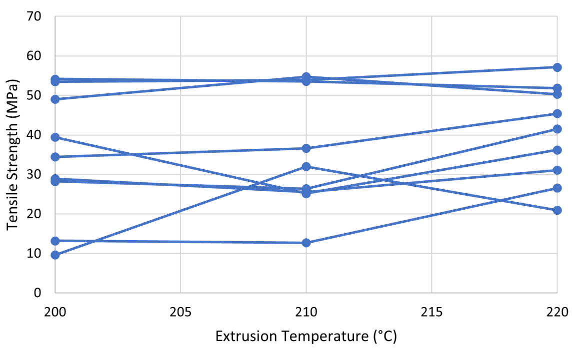

(c) Tensile strength versus extrusion temperature

Figure 6. Parameter effects on tensile strength.

between 200 °C and 210 °C; however, a noticeable upwards trend can be seen between 210 °C and 220 °C.

C. Parameter Correlation

The data from Table IV was given to Eureqa for the GP, resulting in (3) with α in radians, w in mm, and T in $°C$.

$$\sigma_{UTS}(\alpha, w, T) = 53.59 + 5.614 \sin(98.57 \cdot wT \cos\alpha) + wT \cos\alpha - 268.6 \cdot w \cos\alpha \quad (3)$$

The solution details are outlined in Table V, showing (3) achieved the target R^2 value and a maximum error of 5.86 MPa. Fig. 7 shows (3) tested against each of the 27 samples, showing where the error occurs. Results from GP shows good agreement.

TABLE V
GP SOLUTION EVALUATION BASED ON TENSILE TEST DATA

Solution Assessment	**Value**
R2 goodness of fit	0.952
Correlation coefficient	0.977
Maximum error	5.855 MPa
Mean squared error	9.502 MPa
Mean absolute error	2.346 MPa

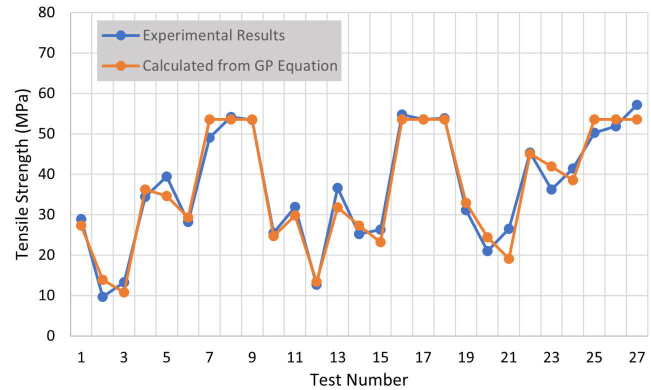

Figure 7. GP solution fit plot.

Once the GP was complete, (3) was set as the objective function, and the GA algorithm was used to explore the responses to the search parameters. GA algorithm was very quickly converged to the maximum tensile strength parameters after about ten generations, shown in Fig. 8. GA predicts the strongest specimens were printed at a high temperature in the direction of loading. The weakest were printed at a low temperature perpendicular to the direction of loading.

VI. Conclusion

GA and GP optimization methods successfully created a predictive model from experimental data gathered from PLA

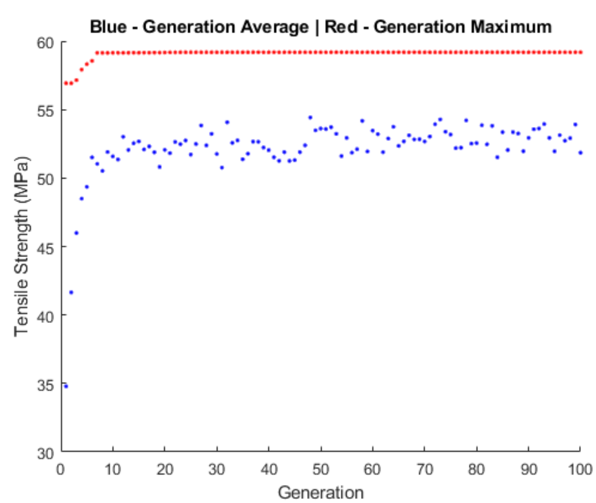

Figure 8. Average and maximum tensile strength over generations.

TABLE VI
BEST PRINTING PARAMETERS AS DETERMINED BY GA

Parameters	Value
Raster angle	90.0°
Extrusion width	0.509 mm
Extrusion temperature	220.0°C
Predicted tensile strength	59.199 MPa

tensile tests. Of the three examined printing parameters, the raster angle was shown to have the greatest impact, followed by extrusion temperature. Extrusion width was found to have little effect on strength but negatively impacted test consistency.

The proposed scheme was highly effective at predicting material properties from varying printing parameters. This has circumvented the current gap in the literature, where there is not yet a powerful general mathematical model for predicting the mechanical behavior of AM parts. Printing parameters can then be optimized without needing a mathematical and mechanical model. Despite being built from limited experimentation and limited varying printing parameters, the proposed scheme is a good step towards building prediction models with many more complex printing parameters. Future research shows promise for considering many more print parameters and expanding parameter ranges. Optimizing multiple competing objective functions is also possible, such as optimizing infill patterns to maximize strength. At the same time, reduce weight or optimize printing speed, print temperature, and print resolution to obtain the best surface finish while reducing print time.

REFERENCES

[1] V. Ana, G. Ferdinando, R. Alexander, and H. Kevin, "Advances in Metal Additive Manufacturing: A Review of Common Processes, Industrial Applications, and Current Challenges," Applied sciences, vol. 11, no. 1213, p. 1213, 2021, doi: 10.3390/app11031213.

[2] U. M. Dilberoglu, B. Gharehpapagh, U. Yaman, and M. Dolen, "The Role of Additive Manufacturing in the Era of Industry 4.0," Procedia Manufacturing, vol. 11, pp. 545-554, 2017/01/01/ 2017, doi: https://doi.org/10.1016/j.promfg.2017.07.148.

[3] M. Yakout, S. C. Veldhuis, and M. A. Elbestawi, "A Review of Metal Additive Manufacturing Technologies," Solid state phenomena, vol. 278, pp. 1-14, 2018, doi: 10.4028/www.scientific.net/SSP.278.1.

[4] S. Chen, "Investigation of FEM numerical simulation for the process of metal additive manufacturing in macro scale," 2019.

[5] A. Jaisingh Sheoran and H. Kumar, "Fused Deposition modeling process parameters optimization and effect on mechanical properties and part quality: Review and reflection on present research," Materials today : proceedings, vol. 21, pp. 1659-1672, 2020, doi: 10.1016/j.matpr.2019.11.296.

[6] S.-H. Ahn, M. Montero, D. Odell, S. Roundy, and P. K. Wright, "Anisotropic material properties of fused deposition modeling ABS," Rapid prototyping journal, vol. 8, no. 4, pp. 248-257, 2002, doi: 10.1108/13552540210441166.

[7] D. P. Cole, J. C. Riddick, H. M. Iftekhar Jaim, K. E. Strawhecker, and N. E. Zander, "Interfacial mechanical behavior of 3D printed ABS," Journal of applied polymer science, vol. 133, no. 30, p. n/a, 2016, doi: 10.1002/app.43671.

[8] B. Huang and S. Singamneni, "Raster angle mechanics in fused deposition modelling," Journal of composite materials, vol. 49, no. 3, pp. 363-383, 2015, doi: 10.1177/0021998313519153.

[9] E. Ulu, E. Korkmaz, K. Yay, O. Burak Ozdoganlar, and L. Burak Kara, "Enhancing the Structural Performance of Additively Manufactured Objects Through Build Orientation Optimization," Journal of mechanical design (1990), vol. 137, no. 11, p. 111410, 2015, doi: 10.1115/1.4030998.

[10] J. Torres, M. Cole, A. Owji, Z. DeMastry, and A. P. Gordon, "An approach for mechanical property optimization of fused deposition modeling with polylactic acid via design of experiments," Rapid prototyping journal, vol. 22, no. 2, pp. 387-404, 2016, doi: 10.1108/RPJ-07-2014-0083.

[11] W. Wang, H. Shao, X. Liu, and B. Yin, "Printing Direction Optimization Through Slice Number and Support Minimization," IEEE access, vol. 8, pp. 75646-75655, 2020, doi: 10.1109/ACCESS.2020.2980282.

[12] V. H. Nguyen, T. N. Huynh, T. P. Nguyen, and T. T. Tran, "Single and Multi-objective Optimization of Processing Parameters for Fused Deposition Modeling in 3D Printing Technology," International journal of automotive and mechanical engineering, vol. 17, no. 1, pp. 7542-7551, 2020, doi: 10.15282/ijame.17.1.2020.03.0558.

[13] J. H. Holland, Adaptation in Natural and Artificial Systems: An Introductory Analysis with Applications to Biology, Control and Artificial Intelligence. MIT Press, 1992.

[14] K. A. De Jong, "AN ANALYSIS OF THE BEHAVIOR OF A CLASS OF GENETIC ADAPTIVE SYSTEMS," ed: ProQuest Dissertations Publishing, 1975.

[15] J. E. Baker, "Adaptive Selection Methods for Genetic Algorithms," presented at the Proceedings of the 1st International Conference on Genetic Algorithms, 1985.

[16] D. E. Goldberg, "Sizing Populations for Serial and Parallel Genetic Algorithms," presented at the Proceedings of the 3rd International Conference on Genetic Algorithms, 1989.

[17] D. Whitley, "The GENITOR algorithm and selection pressure: why rank-based allocation of reproductive trials is best," presented at the Proceedings of the third international conference on Genetic algorithms, George Mason University, USA, 1989.

[18] J. R. Koza, "Non-linear genetic algorithms for solving problems," ed: Google Patents, 1990.

[19] M. Schmidt and H. Lipson, "Eureqa," Version 1.24, 2015. [Online]. Available: https://www.creativemachineslab.com/eureqa.html.